Heterogeneous & Homogeneous & Bio- & Nano-

CHEMCATCHEM

CATALYSIS

Accepted Article

Title: Mn(III) Porphyrins: Catalytic Coupling of Epoxides with CO_2 under Mild Conditions and Mechanistic Considerations

Authors: Jorge Luiz Sônego Milani, Alexandre Moreira Meireles, Werberson de Almeida Bezerra, Dayse Carvalho da Silva Martins, Danielle Cangussu, and Rafael Pavão das Chagas

To be cited as: *ChemCatChem* 10.1002/cctc.201900745

Link to VoR: http://dx.doi.org/10.1002/cctc.201900745

A Journal of ChemPubSoc Europe

WILEY-VCH

www.chemcatchem.org

Mn(III) Porphyrins: Catalytic Coupling of Epoxides with CO_2 under Mild Conditions and Mechanistic Considerations

Jorge Luiz Sônego Milani,*[a] Alexandre Moreira Meireles,[b] Werberson de Almeida Bezerra,[c] Dayse Carvalho da Silva Martins,*[b] Danielle Cangussu[c] and Rafael Pavão das Chagas*[c]

Abstract: A series of 5,10,15,20-tetrakis(2,3-dichlorophenyl)porphyrinate complexes of manganese(III) [Mn^{III}(T2,3DCPP)X] with six different axial ligands (X = NO_3^-, AcO^-, IO_3^-, Br^-, Cl^-, HO^-) were investigated as catalysts in the cycloaddition reactions of CO_2 and styrene oxide (SO), under mild conditions, i.e., atmospheric pressure and 60 °C. [Mn^{III}T(2,3DCPP)IO_3] showed the best catalytic performance, selectively producing the respective cyclic carbonate from diverse epoxides using tetrabutylammonium bromide as a nucleophile source. Mechanistic considerations were inferred from electronic spectra and spectrophotometric titrations, showing that there are a series of equilibriums involved in the formation of the catalytic active species. Stability constants for the proposed equilibrium models were determined using SQUAD software. A catalytic cycle has been proposed based on those observations.

Introduction

Concerns about the increasing high levels of carbon dioxide in the atmosphere and about the dependence of finite fossil carbon resources to produce important chemicals have boosted the interest in catalytic conversion of CO_2. Carbon dioxide may be employed as an abundant, cheap, renewable, non-toxic and non-flammable C1 building block.[1] The thermodynamic stability of CO_2, however, restricts its use as a feedstock in industrial attractive processes.[2] Therefore, the development of catalytic systems to chemically convert CO_2 to useful bulk commercial products is an important topic of research.

Diverse metal- and organo-catalysts have been described to catalytically transform CO_2.[2-3] One of the most studied reactions using CO_2 is its cycloaddition with epoxides to produce cyclic carbonates.[4] Cyclic carbonates have been used as polar aprotic solvents in chemical process, electrolytes in lithium-ion batteries and intermediates to synthesize diols, polycarbonates and polyurethanes.[5]

Under high pressure, complexes either with main-group elements[6] or *d*-block metals[7] show excellent catalytic activity and selectivity, with high TON and TOF values, in the cycloaddition of epoxides with CO_2. However, the conversion of CO_2 through efficient, selective and green catalysis, in mild conditions, remains challenging. The synthesis of cyclic carbonates is one of the few reactions that may employ CO_2 in mild conditions.[8] Examples of catalytic systems in mild conditions include binary (concomitant use of a Lewis acid and a nucleophile source to open the epoxide) and bifunctional systems (a single catalyst species containing Lewis acid and nucleophilic moieties).[7d, 9] Among these systems, heterocyclic macrocycle metal complexes, such as metalloporphyrins[10] and metallocorroles,[8b, 11] are promising catalysts due to the possibility of altering electronic and steric characteristics by modifications of its framework.[12] Also, in square pyramidal metalloporphyrins the axial counterion may influence the stability and catalytic activity and additionally can be readily replaced.[10c, 13]

Metalloporphyrins (MP) have been studied lately for this transformation and some outstanding results were reported.[10a, 14] Bai et al.[15] observed that the nature of axial counter ion changes the Lewis acidity in metal center of the aluminum porphyrin, affecting directly the conversion to cyclic carbonates. Electronic effects in phenyl groups in cobalt porphyrins were studied by Rieger and co-workers.[16] It was observed that electron-withdrawing or electron-donating groups in *para* position of the *meso*-aryl substituents of the macrocycle core can modify significantly the conversion and the selectivity of the system. Also, substituents in the aryl group of the *meso* positions of porphyrin macrocycle are beneficial for this type of reaction.[11] In second-generation metalloporphyrins, the presence of halogen on the *meso*-aryl turns the metal ion coordinated in the macrocycle more acidic, facilitating the epoxide activation.[10c],[11]

In this sense, we have previously reported the synthesis and characterization of new [Mn^{III}(T2,3-DCPP)X] porphyrins (X = Br^-, Cl^-, NO_3^-, AcO^-, HO^-, and IO_3^-, designed as **MnP1-6**, respectively) derived from 5,10,15,20-tetrakis(2,3-dichlorophenyl)porphyrin, (H_2T2,3DCPP) (Figure 1) and described their catalytic behavior in the cycloaddition of CO_2 and epoxides, at high pressure conditions.[17] It was observed that under 5 bar of pressure, the system **MnP2**/tetrabutylammonium bromide was very active converting 74% of styrene oxide in styrene carbonate. Driven by this observation, we decided to conduct studies on the performance of the **MnP1-6** porphyrins under milder conditions, using lower temperatures and atmospheric pressure of CO_2. Herein, it is reported this catalytic studies in the cycloaddition reaction of CO_2 with epoxides, in mild conditions, showing that the binary system **MnP1-6**/TBAB is

[a] Prof. Dr. J. L. S. Milani
Departmento de Química – Instituto de Ciências Exatas
Universidade Federal de Juiz de Fora
Juiz de Fora – MG – Brazil
E-mail: jorge.milani@ufjf.edu.br
[b] M.Sc. A. M. Meireles, Prof. Dr. D. C. S. Martins
Departmento de Química – Instituto de Ciências Exatas
Universidade Federal de Minas Gerais
Belo Horizonte – Mg – Brazil
E-mail: daysequimica@ufmg.br
[c] W. A. Bezerra, Prof. Dr. D. Cangussu, Prof. Dr. R. P. Das Chagas
Instituto de Química
Universidade Federal de Goiás
Goiânia – GO – Brazil
E-mail: rpchagas@ufg.br

Supporting information for this article is given via a link at the end of the document.

very efficient in atmospheric pressure of CO_2 to produce cyclic carbonates.

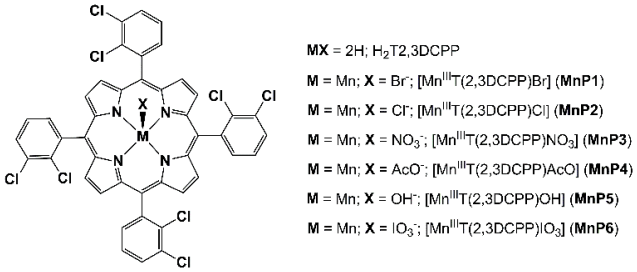

Figure 1. Structure of the metalloporphyrin catalysts.

Additionally, extensive UV-Vis spectroscopic studies have been conducted and detailed equilibriums of the ligand exchange and mechanism pathways have been proposed. Despite the fact that mechanistic considerations have been done to explain the coupling of CO_2 and epoxides,[10c, 15, 18] further efforts are necessary to describe the intricate ligand exchange equilibriums presumably involved in the systems catalyzed by metalloporphyrins.

Results and Discussion

Catalytic studies on the cycloaddition reaction

Metalloporphyrins **MnP1-6** were tested as catalysts, combined with tetrabutylammonium bromide (TBAB) as a nucleophile source, for the coupling reaction between CO_2 and epoxides to form cyclic carbonates, in a solvent-free process under 1 atm. In a general procedure, a 10 mL glass round-bottom flask was charged with catalyst, TBAB and the epoxide. Carbon dioxide was purged into the flask and a CO_2 balloon was connected to maintain 1 atm of pressure.

In an initial screening, all metalloporphyrins MnP1-6 were active to produce styrene carbonate from CO_2 and styrene oxide (SO) without diol formation in standard conditions: 0.01 mol% of metalloporphyrin, 1 mol% of TBAB, and 60 °C (Table 1). The conversions were evaluated in 6, 24 and 48 hours. In short reaction times, conversions were similar, however, in longer experiments, the differences in the activity are increasingly significant. This shows the influence of ligand axial X on the stabilization of the reaction intermediates, affecting the reaction kinetics.

As previously reported, the axial ligand **X** plays a very important role in such catalytic systems. Qin et al.[14d] observed that the electronegativity of the axial ligands favored an increase in the electrophilicity of aluminum metal center leading to larger conversions. Anderson et al.[16] concluded that the lability of ligand **X** is important for the reaction outcome when studying Co(III)-porphyrins with electron-donating and withdrawing groups in the porphyrin ring. In our case, the oxyanions had a better performance on the catalytic systems, and the order of activity is as follow: IO_3^- (**MnP6**) ≅ HO^- (**MnP5**) > AcO^- (**MnP4**) > NO_3^- (**MnP3**) > Cl^- (**MnP2**) > Br^- (**MnP1**). Since Mn(III) is strongly oxophilic in this oxidation state, the oxyanions can provide a good stabilization of the metallic center.[19] Furthermore, all oxygen atoms in the oxyanions are very electronegative and let the manganese cation with a high Lewis acidity, favoring the epoxide activation through Mn-O coordination.[20]

Table 1. Cycloaddition reactions using **MnP1-6**.

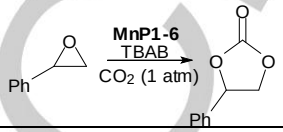

Entry	Catalyst	Time (h)	Conversion (%)[a]	TON[b]	TOF[c]
1	**MnP1**	6	17	1,721	287
2	**MnP1**	24	25	2,494	104
3	**MnP1**	48	36	3,584	75
4	**MnP2**	6	15	1,546	258
5	**MnP2**	24	26	2,577	107
6	**MnP2**	48	39	3,876	81
7	**MnP3**	6	22	2,174	362
8	**MnP3**	24	30	3,049	127
9	**MnP3**	48	40	3,984	83
10	**MnP4**	6	18	1,751	292
11	**MnP4**	24	30	3,040	127
12	**MnP4**	48	46	4,566	95
13	**MnP5**	6	22	2,217	370
14	**MnP5**	24	33	3,322	138
15	**MnP5**	48	49	4,902	102
16	**MnP6**	6	23	2,257	376
17	**MnP6**	24	38	3,759	157
18	**MnP6**	48	50	5,025	105
19	**MnP6**	96	54	5,376	56
20	**MnP6**	120	60	6,024	50
21	[d]	24	14	-	-

Reactions conditions: 0.0025 mmol catalyst (0.01 mol%), 0.25 mmol TBAB (1 mol%), SO (25.00 mmol), Temperature = 60 °C. [a] Conversions determined on basis of ^{1}H NMR analysis. [b] Turnover number (mol of carbonate produced/mol catalyst). [c] Turnover frequency (TON h^{-1}). [d] Blank experiment: only TBAB (1 mol%), SO (25.00 mmol), temperature = 60 °C.

The metalloporphyrin catalyst is inactive in the absence of a cocatalyst, as previously reported under high pressure conditions.[17] In a blank experiment using only TBAB, i.e., without metalloporphyrin catalyst, conversion was 14% in 24 hours (Entry 21, Table 1). In the same conditions, all catalysts led to better conversions and catalyst **MnP6** was the most active converting 38% of SO. Additional experiments using **MnP6** were conducted in 96 and 120 hours and a reasonable conversion of 60% was obtained (Entry 20, Table 1).

Catalyst **MnP6** was chosen to verify the influence of other parameters on the system, including temperature, time, catalyst loading and amount of a range of nucleophile sources. Initially, temperature studies were conducted and provided interesting behavior. At ambient conditions (1 bar and 30 °C) only 4% of styrene oxide was converted to carbonate in 24 hours (Entry 22, Table 2). Increasing temperature improves the conversion values up to 60 °C, which was the optimal temperature,

converting 38% of SO in 24 h (Entry 25, Table 2). At higher temperatures (70 °C, 100 °C and 120 °C) conversions were lower (28, 24 and 25%, respectively; entries 26-28). When the temperature is increased in atmospheric conditions ($P_{[CO2]}$ = 1 bar) two properties are affected: activation barrier (E_a or $\Delta G^{\ddagger}$) and CO_2 solubility. In higher temperatures, CO_2 solubility is diminished, therefore, the cyclic carbonate formation in 70, 100 and 120 °C was similar due to an equilibrium between CO_2 solubility and kinetic effects, both being strongly affected by temperature changes.

Table 2. Cycloaddition reaction using **MnP6/SO**.

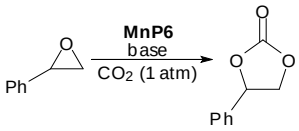

Entry	T (°C)	time (h)	Conversion (%)[a]	TON[b]	TOF[c]
22	30	24	4	411	17
23	40	24	6	647	27
24	50	24	12	1,188	49
25	60	24	38	3,759	157
26	70	24	28	2,793	116
27*	100	24	24	2,392	100
28*	120	24	25	2,481	103
29[d]	60	24	28	1,389	58
30[d]	60	48	47	2,370	49
31[d]*	60	96	73	3,650	38
32[d]*	60	120	87	4,348	36
33[e]	60	24	16	3,190	133
34[f]	60	24	0	-	-
35[g]	60	24	0	-	-
36[h]*	60	24	16	1,558	65
37[i]*	60	24	8	816	34
38[j]	60	24	26	2,625	109
39[k]	60	24	10	974	41
40[l]	60	24	14	1,385	58
41[m]	60	24	21	2,119	88
42[n]	60	24	15	1,508	63
43[n]	60	72	37	3,731	52
44[n]*	60	96	44	4,367	45
45[n]*	60	120	54	5,435	45
46[o]	60	24	0	-	-

Reactions conditions: 0.0025 mmol catalyst (0.01 mol%), 0.25 mmol tetrabutylammonium bromide, TBAB, (1 mol%), SO (25.00 mmol), Temperature = 60 °C. [a] Conversions determined on basis of ^{1}H NMR analysis. [b] Turnover number (mol of carbonate produced/mol catalyst). [c] Turnover frequency (TON h^{-1}). [d] 0.02 mol% of catalyst. [e] 0.005 mol% of catalyst. [f] 1-methyl-imidazole. [g] 4-dimethylaminopyridine (DMAP). [h] Bis(triphenylphosphine)iminium chloride (PPNC). [i] Tetrabutylammonium chloride (TBAC). [j] Tetrabutylammonium iodide (TBAI). [k] 0.25 mol% TBAB (0.0625 mmol). [l] 0.50 mol% TBAB (0.125 mmol). [m] 2.00 mol% TBAB (0.500 mmol). [n] 4 mol% (1 mmol of water). [o] Blank experiment without TBAB. * Diol was observed as a byproduct.

An important consideration in high-temperature reactions (entries 27 and 28) is that diol is produced as a co-product (21 and 32%, respectively); however, in milder conditions (T < 70 °C) no diol is detected in NMR spectra (Figure 2), even when reaction is conducted in presence of water. Experiments conducted with 4 mol% of water at 60 °C (entries 42- 45, Table 2), did not produce any diol, showing selectivities higher than 99%.

Besides temperature, it was also observed that diol production is time-dependent (see entries 29-32 and 42-45, Table 2). It could be expected that epoxide and carbonate might be competing for the Mn axial vacancy site, but not the diol. Since no diol production is observed in initial stages of the reaction, it is assumed that its formation is a result of carbonate degradation.[21] Thus, selectivity may be affected in longer reactions and higher temperatures due to degradation of carbonate to form diol. On the other hand, in temperatures below 70 °C, even in presence of water, selectivity is high showing the robustness of our system in mild conditions.

Nitrogenated bases did not perform the reaction (entries 34 and 35, Table 2), presumably because of the high coordination ability of 1-methylimidazole and DMAP.[15, 18c, 22] Metalloporphyrins **MnP1-6** are five-coordinated complexes with a square pyramidal geometry (Figure 1), so there is a free vacant site at the metallic center where the epoxide should coordinate to suffer the cycloaddition. When 1-methylimidazole and DMAP are in the system, there is a competition between the base and epoxide; the more favorable and strong coordination between Mn(III) and nitrogen donor ligands[12a] turns the active catalyst in a hexacoordinated dormant species and no conversion is observed (see mechanistic considerations).

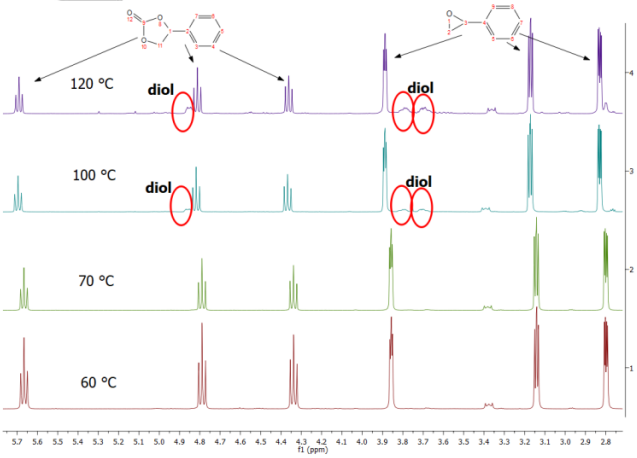

Figure 2. ^{1}H NMR spectra of entries 25, 26, 27, 28 and 42. The ^{1}H NMR (500 MHz) were recorded in $CDCl_3$ with tetramethylsilane (TMS) as an internal reference at room temperature.

The activity of the tetrabutylammonium salts used as nucleophile source cocatalysts varies as follow: TBAB > TBAI > TBAC. Two factors are important when comparing the influence of quaternary ammonium salts: nucleophilicity and leaving group ability. The first is related to the nucleophilic attack to open the epoxide ring and the second is related to the carbonate closure by nucleophilic attack of Mn-O bond in the electrophilic carbon attached to the halogen. The nucleophilicity and leaving group ability order are inverse and by the results, we can speculate,

actually, that a balance between these properties makes TBAB the best cocatalyst in the systems. [23]

When using PPNC and TBAC, which generate the same nucleophilic chloride anion, the conversions were significantly different (entries 36 and 37, Table 2), indicating that the cation nature may affect the system.[18f] The selectivity of the reaction was also affected by the nature of the cocatalyst. By using TBAB or TBAI, no diol was detected (entries 25 and 38, Table 2), however, when the cocatalyst is TBAC or PPNC (entries 36 and 37, Table 2), diol production was attested from NMR (Figure 3). The basicity of anions is determinant for the conversion of cyclic carbonate in diol, as previously reported. [24]

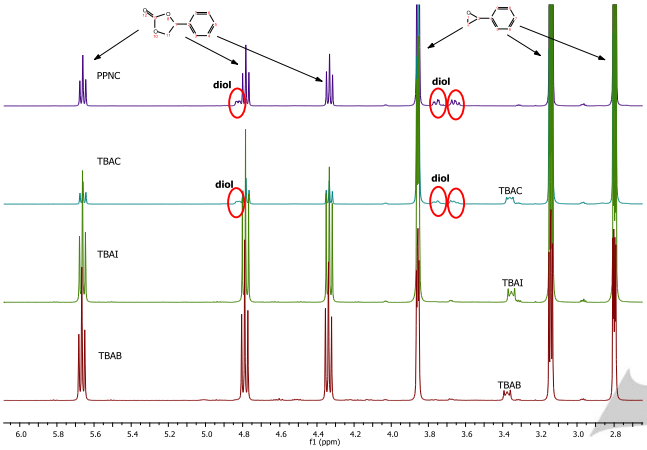

Figure 3. ^{1}H NMR spectra of entries **25**, **38**, **37** and **36**. The ^{1}H NMR (500 MHz) were recorded in $CDCl_3$ with tetramethylsilane (TMS) as an internal reference at room temperature.

Surprisingly, increasing the amount of catalyst (from 0.01 mol% to 0.02 mol%) results in lower conversions after 24 and 48 hours. In 96 and 120 hours, conversions were lower in experiments with 0.01 mol% of catalyst, probably because the decomposition of active species affects more the reaction with lower catalyst load (compare entries 17-20 in Table 1 and entries 29-32 in Table 2).

When the amount of the cocatalyst was changed to 0.25 and 0.50 mol% (entries 39 and 40, Table 2), it was observed a significant decrease in the conversion as expected, since there is a reduction of nucleophilic species to open the epoxide ring. Unexpectedly, when increasing the cocatalyst to 2.00 mol% (entry 41, Table 2), the conversion was also lower compared to 1 mol% of TBAB. This can be attributed to a formation of a dormant species in higher concentrations of bromide anion.

Thereafter, **MnP6** was tested in the cycloaddition of carbon dioxide with a series of epoxides (Figure 4), under the optimized conditions. All epoxides were converted to their corresponding cyclic carbonates with good catalytic activity. The reaction with epoxide glycidol (not presented) resulted in a complex mixture of products, probably due to its susceptibility to polymerization.[9b]

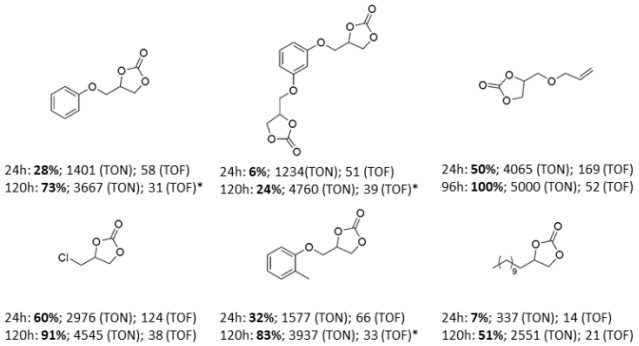

Figure 4. Cycloaddition reaction using **MnP6** with different epoxides, in 24 and 120 hours, under 1 bar of CO_2. Reactions conditions: 0.0025 mmol Mn catalyst (0.02 mol%), 0.25 mmol TBAB (1 mol%), epoxide (12.50 mmol). The conversions were determined on basis of ^{1}H NMR analysis, TON = Turnover number (mol of carbonate produced/mol catalyst), TOF = Turnover frequency (TON h^{-1}). * Diol was formed as a byproduct.

Electronic spectra and mechanistic considerations

Spectrophotometric titrations: stability constants

Metalloporphyrins (MP) contains four nitrogen atoms bound to the metallic center in the macrocyclic plane. In many cases, MP may exhibit axial ligands (L), above and/or below of this, completing the coordination sphere of the metal ion. The number of axial ligands (n) and the stability constants (K_x) can be determined by spectrophotometric measurements, in which the absorbance of one (or more) species is dependent of the ligand and MP concentrations. Equations (1) and (2) represent the formation of two main species, where X is iodate axial ligand.

$$MPX + \mathbf{L} \rightleftharpoons MP(\mathbf{L}) + X \qquad \beta_1 = K_1 \qquad \text{(equation 1)}$$

$$MP(\mathbf{L}) + \mathbf{L} \rightleftharpoons MP(\mathbf{L})_2 \qquad \beta_2 = K_1 \times K_2 \qquad \text{(equation 2)}$$

It is important to note that in equation 1 the product may be either the six-coordinate MPXL or the five-coordinate MPL, which is dependent on both the coordinating ability of the axial ligand X and the dielectric constant of the solvent, factors that affect the dissociation of X.[25] Titration experiments were performed by using CH_2Cl_2 as solvent at 25 ^{o}C in order to ensure that the catalyst and the axial ligands were soluble and available to interact with each other excluding the competition of a coordinating solvent, such as the epoxide.

Titrations of [Mn^{III}(T2,3DCPP)IO_3] (**MnP6**) with TBAB or DMAP showed different behaviors. For TBAB as the titrant, UV-vis spectra exhibited, initially, a hypsochromic shift of the Soret band (band V) in 477 nm, followed by a bathochromic shift to 485 nm. Addition of DMAP as titrant led to a small hyperchromic shift followed by a hypochromic-hypsochromic shift of the Soret Band to 468 nm (Figure 5). These spectral variations suggest the coordination of these ligands, independently, to **MnP6**. The absence of clear isosbestic points in the UV-Vis spectra, at the course of the titration, may indicate the formation of more than

two absorbing species in solution, such as MPX, MPXL, MPL and MPL_2. Thus, the Fortran-based software "*Stability Quotients from Absorbance Data*" (SQUAD), becomes the best option to calculate the more reliable stability constants for proposed equilibrium models from spectrophotometric data.[26]

The best fit of SQUAD was observed when $[Mn^{III}(T2,3DCPP)(L)]IO_3$ and $[Mn^{III}(T2,3DCPP)L_2]$ were considered in the equilibrium model, for both ligands used in titrations experiments. Other tested models led to either non-convergence or significantly inferior fits to the experimental data. Table 3 lists the formation constants and statistical parameters generated by SQUAD for the equilibrium model proposed. The parameters $\Sigma(Obsvd\text{-}Calc)^2$ and α_{data}, which assess the reliability of the proposed model, are within acceptable limits.[26]

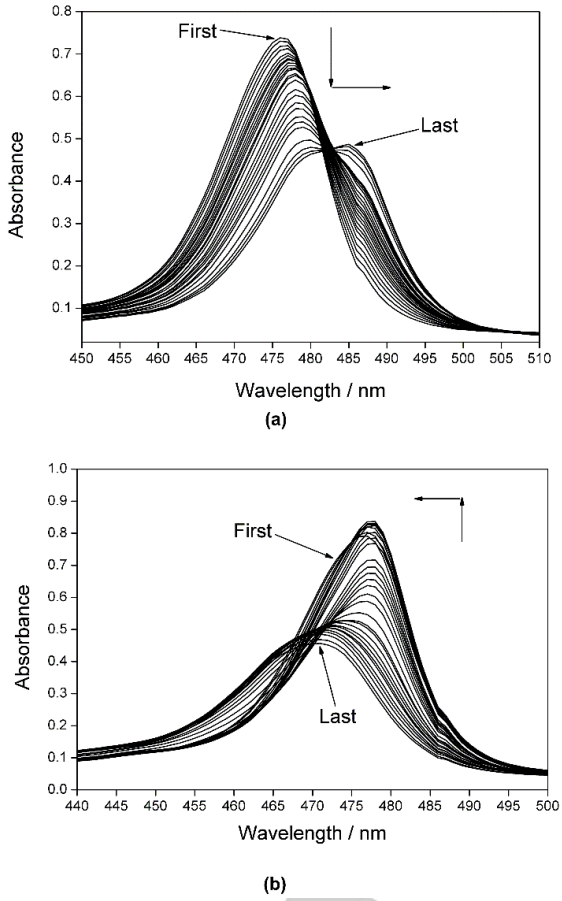

Figure 5. Spectral shifts for the absorbance changes during spectrophotometric titration of the **MnP6**, in CH_2Cl_2 solution, with (a) TBAB, and (b) DMAP.

The output data from SQUAD also includes the molar absorptivities of each species present in solution, in the range of wavelengths considered (Figure S1 and S4, Supplementary Material). For the **MnP6** species was observed a good correlation between the molar absorptivities obtained experimentally (CH_2Cl_2) and those calculated by the SQUAD, indicating excellent reliability of the equilibrium data calculated from the proposed models.

The presence of eight chlorine atoms in the aryl groups at *meso*-positions of **MnP6** makes the Mn(III) ion more electrophilic, favoring the coordination of axial ligands.[27] The higher stability constants with bromide (from TBAB) may be explained by the electron withdrawing effect of the chlorine atoms and by the strong electrostatic interaction[28] between coordinated Mn(III) and bromide ligand. This argument also may justify the coordination of another bromide ligand, leading to an anionic complex *trans*-$[Mn^{III}(T2,3DCPP)Br_2]^-$ in an equilibrium with $[Mn^{III}(T2,3DCPP)Br]$. Chatterjee and Chisholm verified the effect of azide (N_3^-) ligand in [Al^{III}-porphyrins] containing chloride as axial ligand, by IR spectroscopy, and demonstrated the exchange of chloride anion by two azide ligands, leading to anionic complex *trans*-$[Al^{III}\text{-porphyrin}(N_3)_2]^-$.[29] It was also described that the addition of tetrabutylammonium fluoride (TBAF) to a solution of a $[Fe^{III}(TPP)F]$ led to a formation of complex *trans*-$[Fe^{III}(TPP)F_2]^-$.[30] For manganese(III) porphyrins, Chang et al. observed the production of $[Mn^{III}(TPP)(OH)_2]^-$ during the spectrophotometric titration of $[Mn^{III}(TPP)(ClO_4)]$ with tetramethylammonium hydroxide.[31]

Table 3. Parameters obtained by the SQUAD program for the spectrophotometric titration of $[Mn^{III}(T2,3DCPP)IO_3]$ with TBAB or DMAP.[a]

	TBAB	DMAP	TBAB[d]
$\log\beta_1$[b]	6.23	3.54	5.78
$\log\beta_2$[c]	10.17	6.13	9.36
K_1	1.7×10^6	3.4×10^3	4.8×10^5
K_2	8.8×10^3	4.0×10^2	2.7×10^3
K_1/k_2	1.9×10^2	8.4	1.8×10^2
α_{data}	0.003	0.003	0.002
$\Sigma(Obsvd. - Calc)^2$	0.02	0.05	0.008

[a] The titrations were realized in CH_2Cl_2 as solvent. Temperature = 25 °C. [b] $\beta_1 = K_1$; [c] $\beta_2 = K_1 \times K_2$. [d] $[Mn^{III}(TPP)Cl]$ was used in the same conditions employed for $[Mn^{III}(T2,3DCPP)IO_3]$, for comparison.

DMAP exhibited lower values for K_1 and K_2 when compared to TBAB. DMAP is an aminopyridine-type ligand known to be less effective than imidazole-type ligands,[32] although K_1 and K_2 values obtained in this work are comparable to axial coordination of imidazole in second-generation Mn(III)-porphyrins.[12a] This observation could be justified by the resonance effect promoted by the lone electron pair on the amino substituent which makes the pyridinic nitrogen a good σ- and π- donor in DMAP.[32]

Both ligands exhibited higher values for K_1 when compared to K_2, and five- and six- coordinate species (MPXL, MPL and MPL_2) are likely to coexist in solution.[30a] The ratio K_1/K_2 may indicate a preferential tendency to form MPL_2 species. By comparing the K_1/K_2 values for TBAB (1.9×10^2) and DMAP (8.4) it is possible to infer that concentration of six-coordinated complex MPL_2 is higher in presence of DMAP. Boucher[33] mentioned the possibility of neutral N-donor ligands to favor the formation of six-coordinated complexes with $[Mn^{III}(TPP)Cl]$. Bottomley and Kadish[30a], studying the electrochemical properties of $[Fe^{III}(TPP)X]$, described the coordination of two molecules of pyridine or *N,N*-dimethylformamide (DMF) in axial positions of the metal center replacing X ligands. A similar behavior was observed for $[Mn^{III}(TPP)ClO_4]$ in studies of Kelly and Kadish,[25b]

who described that due to the very low coordinating ability of ClO_4^-, coordination of pyridine, imidazole and DMSO occurs in both axial positions of the metal center. The higher ratio K_1/K_2 for TBAB could be justified due to the displacement out-of-plane of Mn(III) ion promoted by the introduction of the first bromide anion,[28] what may hinder the coordination of another bulky bromide ligand in the *trans* position.

For comparison, a simple first-generation metalloporphyrin [Mn^{III}(TPP)Cl] was analyzed in the same conditions employed for the spectrophotometric titration of [Mn^{III}(T2,3DCPP)]IO_3 with TBAB. Similar behavior was observed for [Mn^{III}(TPP)Cl], a hypochromic shift followed to a bathochromic shift of the Soret Band to 485 nm (not shown data). However, this metalloporphyrins exhibited lower $\log\beta_1$ and $\log\beta_2$ (Table 3) when compared to [Mn^{III}(T2,3DCPP)IO_3]. This observation can be justified by the absence of electron-withdrawing atoms in the structure of [Mn^{III}(TPP)Cl], making the Mn(III) ion less electrophilic in this compound.

Mechanistic studies

To obtain further mechanistic details, electronic spectra measurements of **MnP6** in CH_2Cl_2 in the presence of cocatalyst and substrate were performed (Figure 6). Firstly, 5,000 equivalents of SO were added to a solution of **MnP6** 1.16 x 10^{-5} mol L^{-1} and the electronic spectrum remained practically unchanged compared to **MnP6** (Figure 6a and 6b), although SO may eventually be poorly coordinated to manganese center. When TBAB (50 equivalents) was added into the flask, the solution color rapidly changed and a bathochromic shift was observed in all regions of spectra (Figure 6c); at this point, we suppose that there is an equilibrium between species depicted in Scheme 1. Besides, these species may coexist in solution with alkoxide complexes resulting from the epoxide ring-opening (Figure 7). This is evidenced by a shoulder in the Soret band (~470 nm, Figure S11, ESI) that was not observed in blank experiments (**MnP6**/TBAB, Figure 6f and S11, ESI). Tiffner and co-workers[8b] described a similar absorption to support the presence of an axially ligated oxygen in Mn(III) corroles, without assigning to be an alkoxide or a carboxylate.

$$Mn^{III}(T2,3DCPP)IO_3 + TBAB \underset{}{\overset{K_1}{\rightleftharpoons}} [Mn^{III}(T2,3DCPP)Br] + TBA^+\ IO_3^-$$

$$[Mn^{III}(T2,3DCPP)Br] + TBAB \underset{}{\overset{K_2}{\rightleftharpoons}} TBA^+[Mn^{III}(T2,3DCPP)Br_2]^-$$

Scheme 1. Possible equilibria involved in the interaction between [Mn^{III}T(2,3DCPP)IO_3] and TBAB, in CH_2Cl_2.

In the one-hour blank experiment (**MnP6/**TBAB, Figure 6f), the Soret band was observed as a broad band with absorptions at 478 and 484 nm. After 24 hours (Figure 6g), the Soret band appears as a single band with maxima of absorption at 477 nm. The latter UV-Vis spectrum is rather similar to the spectra calculated by the SQUAD for MP**L** specie (Figure S2, ESI), indicating the formation of a more stable [Mn^{III}(T2,3DCPP)Br], so that this absorption only comes from coordination of bromide, without the presence of SO or CO_2.[18d] Thus, it is possible to assume that the ligand exchange depicted in Scheme 1 should be slow as it takes 24 hours for the absorption shift to a single band at 477 nm. Such behavior shows the influence of axial ligand **X** (X = Cl^-, Br^-, NO_3^-, AcO^-, HO^- or IO_3^-) on the reaction conversions, since a more labile Mn(III)-**X** bond would favor a faster ligand exchange to form the more stable species, as attested by the measured stability constants ($\log\beta_2$ = 10.11).

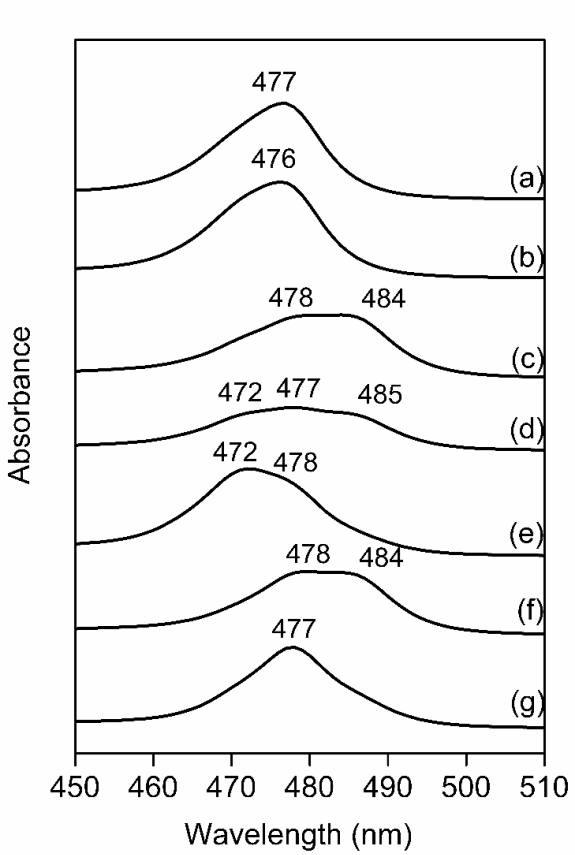

Figure 6. UV-Vis spectra of the changes observed by the interaction between **MnP6** (1.16 x 10^{-5} mol L^{-1}), TBAB (5.80 x 10^{-4} mol L^{-1}, 50 eq.), CO_2 (1 bar) and SO (5.80 x 10^{-2} mol L^{-1}, 5,000 eq.). (a) **MnP6** in CH_2Cl_2; (b) **MnP6** after addition of SO at 25 °C; (c) **MnP6**/SO after addition of TBAB; (d) **MnP6**/SO/TBAB after 1 bar pressure of CO_2 and stirring and 1 h; (e) **MnP6**/SO/TBAB/CO_2 after 24 h; (f) **MnP6** and TBAB, in CH_2Cl_2, after 1 h; (g) **MnP6** and TBAB, in CH_2Cl_2, after 24 h. The UV-Vis spectra could be seen, individually, in ESI (Figures S5-10).

Surprisingly, when the flask was pressurized with 1 bar of CO_2, after one hour, the profile of Soret band changes and appears a "triplet" (472, 477, 485 nm, Figure 6d), indicating an initial CO_2 insertion, leading to the carbonate species coordinated in manganese. At this point, we suggest that the species with inserted CO_2 may coexist with alkoxide species and species depicted in Scheme 1. Within 24 hours the spectrum profile completely changes by a hypsochromic shift, indicating that all active catalytic species had CO_2 inserted into alkoxide-metal bond, which should be a slow step in reactions at 1 bar of pressure. This is evidenced carrying out reactions in lower temperatures (Entries 22-24, Table 2), when conversions were

very low, probably because the transition free energy to the carbonate ring closure should be high.[34] Therefore, the nucleophilic attack by alkoxide bond (O—Mn) in the electrophilic carbon also might be a rate-determining step as can be inferred from UV-Vis analysis.

The influence of axial ligands in the reaction is related to their coordinating ability. The catalytic results exhibited in Table 1 revealed that this is less pronounced in 6 hours (conversions between 15 and 23%); however, in longer periods, as in 48 hours, conversions are rather different (from 36 to 52%). When the epoxide is attacked by an external nucleophile, an alkoxide bond is formed between the Mn(III) and epoxide and, at this point there are at least two possibilities: a) the catalytic species remain neutral and an axial ligand is uncoordinated (five-coordinated), or b) the catalytic species becomes anionic with tetrabutylammonium cation as counterion (six-coordinated). Both pathways may coexist in the catalytic cycle, and the preference for one or another depends on the coordinating ability and lability of axial ligand **X**. Since axial ligand **X** influences on the stabilization of the reaction intermediates, affecting the reaction kinetics, the ligand exchange equilibriums are the responsible for the differences in conversions.

As mentioned above, the ligand exchange depicted in Scheme 1 should be slow, even for the poor coordinating IO_3^- axial ligand (see blank experiment in figure 6f and 6g). Thus, even if the complexes MP**L** and MP$\mathbf{L_2}$ (L = Br^-) have large values of K_1 = 1.7 x 10^6 and K_2 = 8.8 x 10^3 (see section 2.2.1), the [Mn^{III}(T2,3DCPP)X] should be active in the catalytic cycle, since different conversions were observed using different axial ligands. Based on those observations, we propose the catalytic cycle presented in Figure 7. The reaction proceeds upon coordination of SO in the metal center, followed by the TBAB addition. The large excess of TBAB should be able to replace the ligand **X** or the SO coordinated in the manganese center, leading to the many different species, some are dormant however reversible MP$\mathbf{L}_2$ (L = axial ligand, except SO) and active species such as $[MP(SO)]^+$ or MP**L**(SO), the UV-Vis spectra in Figure 6 (and Figure S8, ESI) show the enlargement in Soret band, that characterize the mixture of different metalloporphyrins species.[18d] Subsequently, a nucleophilic attack by a bromide anion from TBAB occur either on α or β carbon of epoxide, preferentially in the less hindered carbon (β attack).[35] However, α attack occur when some fragment of epoxide is electron-withdrawing as a phenyl group in **SO**, but with low selectivity.[36]

The ring-opening reaction is followed by CO_2 insertion and ring-closure to form the respective cyclic carbonate, regenerating the active species. Ema et al.[18f] have studied the binding constants (K_a) for 1,2-epoxyhexene and the respective cyclic carbonate and have verified that the epoxide and cyclic carbonates in Zn(II) and Mg(II)-porphyrins have small values of K_a, measured in CH_2Cl_2. These results indicate that the ligand exchange (cyclic carbonate to epoxide) is not a rate-determining step.[57] By connecting the studies of Ema with the present studies, there are three possible rate-determining steps in the catalytic cycle: epoxide opening, carbon dioxide insertion and ring-closure, to form the cyclic carbonate at 30 °C. The complete understanding of the catalytic system is not trivial because a series of different species may coexist in diverse equilibriums. The lability of axial ligands of the porphyrin complex is responsible for the reaction outcome and for the preferential formation of a five- or hexa-coordinated intermediate (Figure 7).

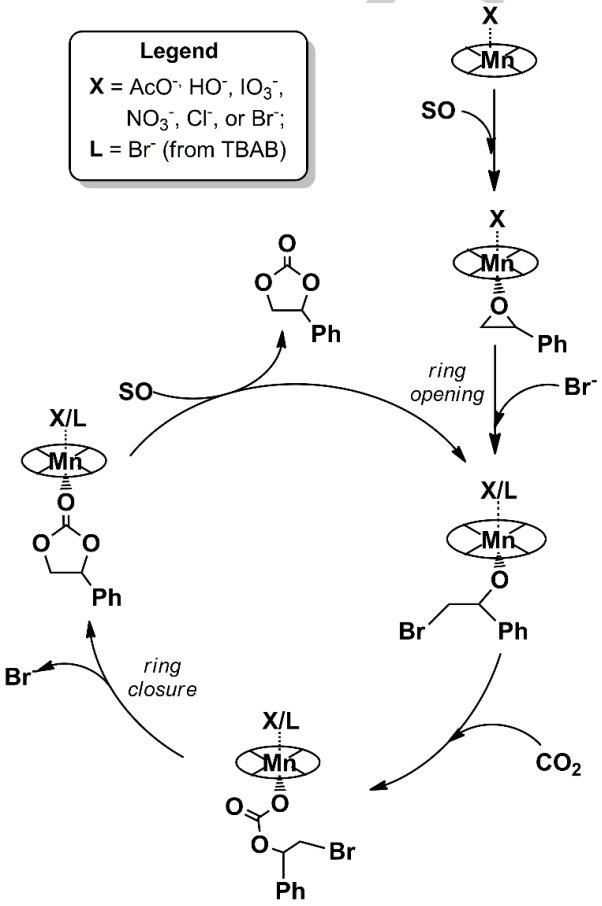

Figure 7. Catalytic cycle proposed for the cycloaddition of CO_2 in SO using [Mn^{III}(T2,3DCPP)**X**] (**X** = Cl^-, Br^-, NO_3^-, AcO^-, HO^- or IO_3^-) and TBAB. Ligand X or L may or may not be coordinated, depending on its nature.

In order to understand the behavior of the system when nitrogenated bases were used instead of TBAX or PPNC, we investigate UV-Vis spectra in the reaction course using DMAP as cocatalyst. DMAP and 1-methylimidazole have been reported as good cocatalysts for copolymerization of CO_2 and epoxides catalysed by metalloporphyrins.[37] In contrast, in our work, reactions performed in the presence of these cocatalysts did not convert SO (Entry 34 and 35, Table 2). According to the spectrophotometric titrations, the successive addition of DMAP led to the formation of [Mn^{III}(T2,3DCPP)(DMAP)]IO_3 and [Mn^{III}(T2,3DCPP)$(DMAP)_2$]IO_3 (Scheme 2).

$$Mn^{III}(T2,3DCPP)IO_3 + NB \overset{K_1}{\rightleftharpoons} [Mn^{III}(T2,3DCPP)(NB)]^+ + IO_3^-$$

$$[Mn^{III}(T2,3DCPP)(NB)]^+ + NB \overset{K_2}{\rightleftharpoons} [Mn^{III}(T2,3DCPP)(NB)_2]^+$$

Scheme 2. Possible equilibria involved in the interaction between [Mn^{III}(T2,3DCPP)IO_3] and different nitrogenated base (NB), in CH_2Cl_2.

Initially SO was added to a solution of **MnP6** in CH_2Cl_2 and no change was observed (Figure 8b). However, when DMAP was added, an enlargement of Soret band was observed (Figure 8c). This enlargement of the Soret band could be admitted to the production of species depicted in Scheme 2, what is corroborated by the spectrophotometric titrations (Figure 6b). Similarly, in blank experiments of **MnP6** in the exclusive presence of DMAP, the UV-Vis spectrum (ESI, Figure S12), exhibited the same enlargement of the Soret band, indicating the coexistence of more than one specie in solution (possibly MP**L** and MP$\mathbf{L_2}$, where **L** = DMAP).

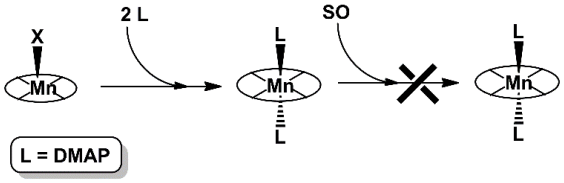

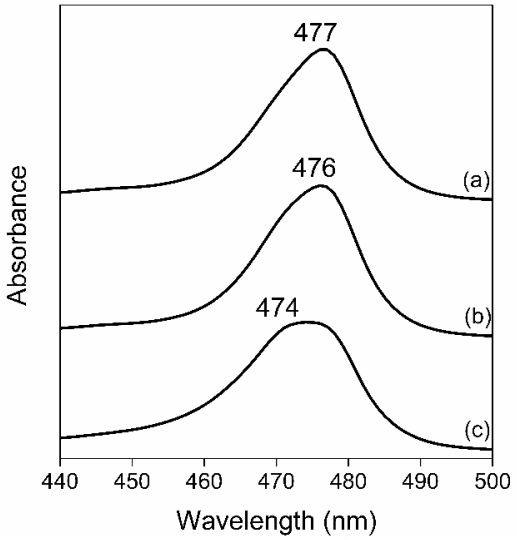

Figure 8. UV-Vis spectra of the changes observed by the interaction between **MnP6** (1.16 x 10^{-5} mol L^{-1}), DMAP (5.80 x 10^{-4} mol L^{-1}, 50 eq.), CO_2 (1 bar) and SO (5.80 x 10^{-2} mol L^{-1}, 5,000 eq.). (a) **MnP6** in CH_2Cl_2; (b) **MnP6** after addition of SO at 25 °C; (c) **MnP6**/SO after addition of DMAP.

It is presumable from our results and previous studies,[25b, 33, 38] that in the presence of a large excess of DMAP, **MnP6** is converted to a six-coordinated species $[MnP(DMAP)_2]X$. The ratio K_1/K_2 calculated from SQUAD was $1.9x10^2$ for TBAB and 8.4 for DMAP (Table 3), indicating a higher tendency to form MPL_2 species when using DMAP. Kelly and Kadish[25b] reported that $[Mn^{III}(TPP)X]$ when dissolved in pyridine produces $[Mn^{III}(TPP)(Py)_2]^+$, when the axial ligand X is a poor coordinating ion as ClO_4^-, I^- or Br^-. In our case, the axial ligand IO_3^- has a very weak coordinating ability and DMAP is an even better ligand than pyridine. Since DMAP is a very good σ- and π-donor, plausibly, the bond Mn-N_{DMAP} is strong and kinetically non-labile, so the formation of an inert MPL_2 species could be admitted as the reason for the inactivation of catalyst in the reactions with DMAP.

When 1-methylimidazole was used as cocatalyst instead of DMAP, similar behavior was observed (0% of conversion). Da Silva and co-workers[12a] have studied similar Mn(III)-porphyrins ($[Mn^{III}(TPP)Cl]$, $[Mn^{III}(APTPP)Cl]$, $[Mn^{III}(Br_9APTPP)Cl]$, $[Mn^{III}(T4CMPP)Cl]$ and $[Mn^{III}(Br_8T4CMPP)Cl]$) in the presence of imidazole as cocatalyst. Similarly, the authors have made a spectrophotometric titration of Mn(III)-porphyrins and calculated K_1 and K_2, in equilibria quite similar to Scheme 2. They observed that MP$\mathbf{L_2}$ species had a larger β value than MP**L** species, what should occur in our case. In general, imidazoles are strong π-donors and, when compared to pyridine derivates, the smaller size of these ligands favors the coordination in metalloporphyrins.[32] This is a strong evidence that 1-methylimidazole coordinate in manganese center inactivating the systems because the resulting complex is kinetically inert to ligand exchange in this condition.

In the case of TBAB, regardless if a five- or six- coordinated intermediate is formed in the catalytic system, the Mn-Br bond seems to be sufficiently labile to exchange with epoxide to initiate the catalytic cycle. While, for DMAP, the production of six-coordinated $MnP(DMAP)_2$ and the non-labile Mn-N_{DMAP} bond prevents the reaction to occur.

Further studies are necessary for a complete understanding of the intricate mechanisms of ligand exchange involved in the binary catalytic systems for the production of cyclic carbonates.

Conclusions

In summary, six manganese porphyrins (**MnP1**-**6**) were tested as catalysts for the cycloaddition of CO_2 and epoxides under mild conditions. A series of parameters was evaluated in the catalytic system and $[Mn^{III}(T2,3DCPP)IO_3]$ (**MnP6**) showed the best performance in the reaction with high selectivity, even in presence of water. It could be used to convert diverse epoxides in cyclic carbonates, converting up to 91% of epichlorohydrin, using very low catalyst and cocatalyst loads (compared to present literature) under atmospheric pressure and 60 °C. The chlorinated aryl substituents on the meso positions of metalloporphyrin may facilitate the initial reaction by enhancing binding interactions among catalyst, cocatalyst and reactant.

Mechanistic considerations were inferred from studies based on UV-Vis spectra and spectrophotometric titration. Stability constants for species derived from **MnP6** and bromide anion or DMAP were determined using SQUAD software. The intermediate $[Mn^{III}(T2,3DCPP)Br_2]^-$, formed when TBAB is used as cocatalyst, presents higher stability constants compared to $[Mn^{III}(T2,3DCPP)(DMAP)_2]^+$, produced when DMAP is used as cocatalyst. The electron withdrawing chlorines drain the electronic charge from the axial ligands and make the anionic $[MPBr_2]$- more stable than cationic $[MP(DMAP)_2]^+$, as can be seen in titration data. Still, the former has labile Mn-Br bonds which is essential for the reaction to occur, whilst the latter is

kinetically inert and no ligand substitution reactions occur after $[Mn^{III}(T2,3DCPP)(DMAP)_2]^+$ is formed in the catalytic system.
A series of ligand exchange equilibriums is involved in the formation of the catalytic active species, what can be presumed by accompanying the reaction with UV-vis spectra. The lability of axial ligand **X** of Mn(III)-porphyrins and of the ligand L (from nucleophile source cocatalyst) determine the coexistence of different species in the process and are the responsible for the reaction outcome. A plausible catalytic cycle has been proposed, supposing that the mechanism may occur via a neutral and an anionic route. This work illustrates the intricacy of the mechanism of homogeneous metallic systems to convert CO_2 and epoxides in carbonates and shed light to some mechanistic aspects of the reaction.

Experimental Section

Reagents

Analytical grade CH_3OH, CH_2Cl_2, $CHCl_3$, *n*-hexane and *N,N*-dimethylformamide were obtained from Aldrich Chemical Co. All the other reagents were of analytical grade and were used without further purification. The CO_2 gas (99.99%) was purchased and used without further purification. TBAB, TBAI, TBAC, PPNC, DMAP, SO, and the other epoxides were used without further purification. Porphyrins were obtained according to published protocol.[17]

Instrumentation

UV-vis spectra were recorded in HP 8453A diode-array spectrophotometer. Solution NMR spectra were collected at ambient temperatures using Bruker Avance III 11.75 Tesla spectrometer (500 MHz) at room temperature in deuterated chloroform ($CDCl_3$) with tetramethylsilane (TMS) as internal reference.

Axial Coordination studies to $[Mn^{III}T(2,3DCPP)IO_3]$

Spectrophotometric titrations were performed in a borosilicate glass cuvette tightly capped with a Teflon-coated silicon septum using a 25.0 ± 0.2 ^oC thermostatized cell-holder. All the stock and working solutions were prepared using dichloromethane as solvent. The initial concentration of the solutions in the cuvette was determined spectrophotometrically by the molar absorptivity (ε) of the Soret band in λ = 477 nm. Aliquots of the stock solution of the titrating ligand (tetrabutylammonium bromide, TBAB, or 4-dimethylaminopyridine, DMAP) were added consecutively to the cuvette through the cuvette silicon septum, with the aid of Hamilton® microsyringes. The system was magnetically stirred for 1 min at 25.0 ± 0.2 ^oC, in order to allow thermal and chemical equilibrium be achieved before recording the UV–vis spectrum. The titration was considered to be complete when UV–vis spectral variations ceased to occur. The mathematical treatment of the data obtained by the titrations was carried with the use of the software *Stability Quotients from Absorbance Data* (SQUAD).[26]

General procedure for cycloaddition reactions

In a general procedure, a 10 mL round flask with a magnetic stirrer was charged with complexes MnP1-6 (0.0025 mmol, 0.0010-0.0013 g, 0.01 mol%), cocatalyst (TBAB, 0.25 mmol, 0.0805 g, 1 mol%) and styrene oxide (25 mmol, 1.75 mL). A balloon of carbon dioxide (1 bar) was pressurized into this mixture and the reaction was operated at the predetermined conditions. After the reaction was completed, the vessel was cooled to room temperature (25-30 °C) and a sample was prepared to ^1H NMR analysis. Conversion was calculated on the basis of ^1H NMR spectroscopy of the crude reaction mixture thus obtained, in deuterated chloroform. Quantities were adjusted when changing the proportions, type of cocatalyst and the epoxide.

Acknowledgements

This work was financially supported by Fundação de Amparo à Pesquisa do Estado de Goiás (Nº 201610267001033), by Fundação de Amparo à Pesquisa do Estado de Minas Gerais (FAPEMIG), by Financiadora de Estudos e Projetos (Finep), and by Conselho Nacional de Desenvolvimento Científico e Tecnológico (CNPq). W.A.B. and A.M.M. thank CNPq for fellowships.

Keywords: Carbon dioxide fixation; Homogeneous catalysis; Metalloporphyrins; Mild conditions; SQUAD.

[1] M. Aresta, *Carbon Dioxide as Chemical Feedstock*, Wiley-VCH, Weinheim, **2010**.

[2] J. Artz, T. E. Muller, K. Thenert, J. Kleinekorte, R. Meys, A. Sternberg, A. Bardow, W. Leitner, *Chem. Rev.* **2018**, *118*, 434.

[3] a) N. A. Tappe, R. M. Reich, V. D'Elia, F. E. Kuhn, *Dalton Trans.* **2018**, *47*, 13281; b) C. M. Kozak, K. Ambrose, T. S. Anderson, *Coord. Chem. Rev.* **2018**, *376*, 565; c) M. Alves, B. Grignard, R. Mereau, C. Jerome, T. Tassaing, C. Detrembleur, *Catal. Sci. Technol.* **2017**, *7*, 2651; d) Q.-W. Song, Z.-H. Zhou, L.-N. He, *Green Chem.* **2017**, *19*, 3707; e) C. Maeda, Y. Miyazaki, T. Ema, *Catal. Sci. Technol.* **2014**, *4*, 1482; f) M. Cokoja, C. Bruckmeier, B. Rieger, W. A. Herrmann, F. E. Kuhn, *Angew. Chem., Int. Ed.* **2011**, *50*, 8510; g) I. Omae, *Catal. Today* **2006**, *115*, 33.

[4] a) A. J. Kamphuis, F. Picchioni, P. P. Pescarmona, *Green Chem.* **2019**, *21*, 406-448; b) H. Buttner, L. Longwitz, J. Steinbauer, C. Wulf, T. Werner, *Top. Curr. Chem.* **2017**, *375*(3), 50; c) C. Martín, G. Fiorani, A. W. Kleij, *ACS Catal.* **2015**, *5*, 1353; d) W. N. R. Wan Isahak, Z. A. Che Ramli, M. W. Mohamed

Hisham, M. A. Yarmo, *Renewable Sustainable Energy Rev.* **2015**, *47*, 93; e) M. North, R. Pasquale, C. Young, *Green Chem.* **2010**, *12*, 1514.

[5] a) A.-A. G. Shaikh, S. Sivaram, *Chem. Rev.* **1996**, *96*, 951; b) B. Schäffner, F. Schäffner, S. P. Verevkin, A. Börner, *Chem. Rev.* **2010**, *110*, 4554; c) J. S. B. Forero, J. A. H. Muñoz, J. J. Junior, F. M. d. Silva, *Curr. Org. Synth.* **2016**, *13*, 834.

[6] a) L. Cuesta-Aluja, J. Castilla, A. M. Masdeu-Bulto, *Dalton Trans.* **2016**, *45*, 14658; b) J. Steinbauer, T. Werner, *ChemSusChem* **2017**, *10*, 3025; c) Y. Chen, R. Qiu, X. Xu, C.-T. Au, S.-F. Yin, *RSC Adv.* **2014**, *4*, 11907; d) D. Tian, B. Liu, Q. Gan, H. Li, D. J. Darensbourg, *ACS Catal.* **2012**, *2*, 2029.

[7] a) A. Buonerba, F. D. Monica, A. D. Nisi, E. Luciano, S. Milione, A. Grassi, C. Capacchione, B. Rieger, *Faraday Discuss.* **2015**, *183*, 83; b) H. Büttner, C. Grimmer, J. Steinbauer, T. Werner, *ACS Sustainable Chem. Eng.* **2016**, *4*, 4805; c) A. Kilic, M. Durgun, E. Aytar, R. Yavuz, *J. Organomet. Chem.* **2018**, *858*, 78; d) R. Ma, L.-N. He, Y.-B. Zhou, *Green Chem.* **2016**, *18*, 226; e) M. Taherimehr, A. Decortes, S. M. Al-Amsyar, W. Lueangchaichaweng, C. J. Whiteoak, E. C. Escudero-Adán, A. W. Kleij, P. P. Pescarmona, *Catal. Sci. Technol.* **2012**, *2*, 2231; f) X.-D. Lang, Y.-C. Yu, L.-N. He, *J. Mol. Catal. A: Chem.* **2016**, *420*, 208.

[8] a) R. R. Shaikh, S. Pornpraprom, V. D'Elia, *ACS Catal.* **2018**, *8*, 419; b) M. Tiffner, S. Gonglach, M. Haas, W. Schöfberger, M. Waser, *Chem. – Asian J.* **2017**, *12*, 1048.

[9] a) J. A. Castro-Osma, M. North, X. Wu, *Chem. - Eur. J.* **2016**, *22*, 2100; b) J. Steinbauer, A. Spannenberg, T. Werner, *Green Chem.* **2017**, *19*, 3769; c) R. Luo, X. Zhou, S. Chen, Y. Li, L. Zhou, H. Ji, *Green Chem.* **2014**, *16*, 1496; d) A. Monfared, R. Mohammadi, A. Hosseinian, S. Sarhandia, P. D. K. Nezhad, *RSC Adv.* **2019**, *9*, 3884.

[10] a) C. Maeda, J. Shimonishi, R. Miyazaki, J. Y. Hasegawa, T. Ema, *Chem. - Eur. J.* **2016**, *22*, 6556; b) J. Peng, Y. Geng, H.-J. Yang, W. He, Z. Wei, J. Yang, C.-Y. Guo, *Mol. Catal.* **2017**, *432*, 37; c) L. Cuesta-Aluja, J. Castilla, A. M. Masdeu-Bultó, C. A. Henriques, M. J. F. Calvete, M. M. Pereira, *J. Mol. Catal. A: Chem.* **2016**, *423*, 489.

[11] P. Li, Z. Cao, *Organometallics* **2018**, *37*, 406.

[12] a) V. S. da Silva, A. M. Meireles, D. C. D. Martins, J. S. Rebouças, G. DeFreitas-Silva, Y. M. Idemori, *Appl. Catal., A* **2015**, *491*, 17; b) D. C. D. Martins, F. C. Silva, A. M. Meireles, É. A. R. Soares, G. D. F. Silva, S. A. Vieira-Filho, L. P. Duarte, J. S. Rebouças, Y. M. Idemori, *Catal. Commun.* **2016**, *86*, 104.

[13] L. Jin, H. Jing, T. Chang, X. Bu, L. Wang, Z. Liu, *J. Mol. Catal. A: Chem.* **2007**, *261*, 262.

[14] a) C. Maeda, S. Sasaki, T. Ema, *ChemCatChem* **2017**, *9*, 946; b) J. Y. Hasegawa, R. Miyazaki, C. Maeda, T. Ema, *Chem. Rec.* **2016**, *16*, 2260; c) C. Maeda, T. Taniguchi, K. Ogawa, T. Ema, *Angew. Chem., Int. Ed.* **2015**, *54*, 134; d) Y. Qin, H. Guo, X. Sheng, X. Wang, F. Wang, *Green Chem.* **2015**, *17*, 2853; e) X. Jiang, F. Gou, C. Qi, *J. CO2 Util.* **2019**, *29*, 134; f) L. He, J. K. Nath, Q. Lin, *Chem. Commun.* **2019**, *55*, 412; g) S. Jayakumar, H. Li, L. Tao, C. Li, L. Liu, J. Chen, Q. Yang, *ACS Sustainable Chem. Eng.* **2018**, *6*, 9237.

[15] D. Bai, S. Duan, L. Hai, H. Jing, *ChemCatChem* **2012**, *4*, 1752.

[16] C. E. Anderson, S. I. Vagin, W. Xia, H. Jin, B. Rieger, *Macromolecules* **2012**, *45*, 6840.

[17] J. L. S. Milani, A. M. Meireles, B. N. Cabral, W. de Almeida Bezerra, F. T. Martins, D. C. da Silva Martins, R. P. das Chagas, *J. CO2 Util.* **2019**, *30*, 100.

[18] a) D. J. Darensbourg, A. I. Moncada, *Inorg. Chem.* **2008**, *47*, 10000; b) J. A. Castro-Osma, M. North, X. Wu, *Chem. - Eur. J.* **2014**, *20*, 15005; c) J. Martinez, J. A. Castro-Osma, A. Earlam, C. Alonso-Moreno, A. Otero, A. Lara-Sanchez, M. North, A. Rodriguez-Dieguez, *Chem. - Eur. J.* **2015**, *21*, 9850; d) J. A. Castro-Osma, K. J. Lamb, M. North, *ACS Catal.* **2016**, *6*, 5012; e) J. A. Castro-Osma, M. North, W. K. Offermans, W. Leitner, T. E. Muller, *ChemSusChem* **2016**, *9*, 791; f) T. Ema, Y. Miyazaki, J. Shimonishi, C. Maeda, J. Y. Hasegawa, *J. Am. Chem. Soc.* **2014**, *136*, 15270; g) R. Huang, J. Rintjema, J. González-Fabra, E. Martín, E. C. Escudero-Adán, C. Bo, A. Urakawa, A. W. Kleij, *Nat. Catal.* **2018**, *2*, 62; h) P. Li, Z. Cao, *Dalton Trans.* **2019**, *48*, 1344.

[19] D. P. Kessissoglou, M. L. Kirk, M. S. Lah, X. Li, C. Raptopoulou, W. E. Hatfield, V. L. Pecoraro, *Inorg. Chem.* **1992**, *31*, 5424.

[20] D. Bai, X. Wang, Y. Song, B. Li, L. Zhang, P. Yan, H. Jing, *Chin. J. Catal.* **2010**, *31*, 176.

[21] F. D. Bobbink, F. Menoud, P. J. Dyson, *ACS Sustainable Chem. Eng.* **2018**, *6*, 12119-12123.

[22] a) L. Jin, T. Chang, H. Jing, *Chin. J. Catal.* **2007**, *28*, 287.

[23] a) J. L. S. Milani, I. S. Oliveira, P. A. D. Santos, A. K. S. M. Valdo, F. T. Martins, D. Cangussu, R. P. D. Chagas, *Chin. J. Catal.* **2018**, *39*, 245; b) W. Wang, C. Li, L. Yan, Y. Wang, M. Jiang, Y. Ding, *ACS Catal.* **2016**, *6*, 6091.

[24] a) M. O. Vieira, W. F. Monteiro, B. S. Neto, R. Ligabue, V. V. Chaban, S. Einloft, *Catal. Lett.* **2018**, *148*, 108; b) J. Sun, X. Yao, W. Cheng, S. Zhang, *Green Chem.* **2014**, *16*, 3297.

[25] a) F. A. Walker, M.-W. Lo, M. T. Ree, *J. Am. Chem. Soc.* **1976**, *98*, 5552; b) S. L. Kelly, K. M. Kadish, *Inorg. Chem.* **1982**, *21*, 3631.

[26] D. J. Leggett, S. L. Kelly, L. R. Shiue, Y. T. Wu, D. Chang, K. M. Radish, *Talanta* **1983**, *30*, 579.

[27] P. Bhyrappa, V. Krishnan, M. Nethaji, *J. Chem. Soc., Dalton Trans.* **1993**, 1901.

[28] L. J. Boucher, *Ann. N. Y. Acad. Sci.* **1973**, *206*, 409.

[29] C. Chatterjee, M. H. Chisholm, *Inorg. Chem.* **2011**, *50*, 4481.

[30] a) L. A. Bottomley, K. M. Kadish, *Inorg. Chem.* **1981**, *20*, 1348; b) P. Gans, J.-C. Marchon, J.-M. Moulis, *Polyhedron* **1982**, *1*, 737-738; c) D. L. Hickman, H. M. Goff, *Inorg. Chem.* **1983**, *22*, 2787.

[31] C.-H. Chang, S.-H. Cheng, Y. O. Su, *J. Chin. Chem. Soc.* **1999**, *46*, 221.

[32] D. Mohajer, G. Karimipour, M. Bagherzadeh, *New J. Chem.* **2004**, *28*, 740.

[33] L. J. Boucher, *Coord. Chem. Rev.* **1972**, *7*, 289.

[34] a) F. Jutz, A. Buchard, M. R. Kember, S. B. Fredriksen, C. K. Williams, *J. Am. Chem. Soc.* **2011**, *133*, 17395-17405; b) I. Sinha, Y. Lee, C. Bae, S. Tussupbayev, Y. Lee, M.-S. Seo, J. Kim, M.-H. Baik, Y. Lee, H. Kim, *Catal. Sci. Technol.* **2017**, *7*, 4375.

[35] D. J. Darensbourg, E. B. Frantz, *Inorg. Chem.* **2007**, *46*, 5967.

[36] G.-P. Wu, S.-H. Wei, X.-B. Lu, W.-M. Ren, D. J. Darensbourg, *Macromolecules* **2010**, *43*, 9202.

[37] H. Sugimoto, K. Kuroda, *Macromolecules* **2008**, *41*, 312.

[38] B. Meunier, M.-E. d. Carvalho, O. Bortolini, M. Momenteau, *Inorg. Chem.* **1988**, *27*, 161.

10.1002/cctc.201900745

WILEY-VCH

FULL PAPER

The coupling of CO_2 with epoxides is catalyzed by Mn(III) porphyrins, under mild conditions, and a series of equilibriums is involved in the formation of the catalytic active species. Electronic spectra and spectrophotometric titrations provided insights into the mechanism of the reaction.

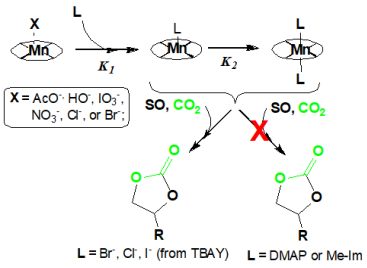

Jorge Luiz Sônego Milani, Alexandre Moreira Meireles, Werberson de Almeida Bezerra, Dayse Carvalho da Silva Martins,* Danielle Cangussu and Rafael Pavão das Chagas**

Page No. – Page No.

Mn(III) Porphyrins: Catalytic Coupling of Epoxides with CO_2 under Mild Conditions and Mechanistic Considerations